RSC Mechanochemistry

ROYAL SOCIETY OF CHEMISTRY

PAPER

View Article Online
View Journal | View Issue

Cite this: *RSC Mechanochem.*, 2024, **1**, 94

Mechanically induced self-propagating reactions (MSRs) to instantly prepare binary metal chalcogenides: assessing the influence of particle size, bulk modulus, reagents melting temperature difference and thermodynamic constants on the ignition time†

Matej Baláž, *[a] Róbert Džunda,[b] Radovan Bureš, [b] Tibor Sopčák[b] and Tamás Csanádi[bc]

Mechanically induced self-propagating reactions (MSRs) offer the possibility to obtain desired products in an ultrafast and thus cost- and energy-efficient manner. In this work, this is demonstrated for ten binary metal chalcogenides (CdS, CdSe, In_2S_3, NiS, NiSe, PbS, PbSe SnSe, ZnS and ZnSe) by processing mixtures of metals and chalcogens in a planetary ball mill for less than 10 minutes. The MSR process for Ni-based systems is reported for the first time. The studied metals reacted much faster with selenium than with sulfur (with the exception of Ni). The successful MSR occurrence was evidenced by an abrupt increase of gas pressure in the milling jar monitored *in situ* and subsequently *ex situ* by X-ray diffraction. The crystallite size of the as-received products was usually in the range 40–260 nm. All the reactions were performed in an air atmosphere, and thus the presence of an inert gas was not necessary. An effort was made to correlate the observed ignition times with the particle size of the precursors, their melting temperature, bulk modulus and thermodynamic parameters ($\Delta H/C_p$ and ΔG). While the thermodynamics does not seem to play an important role here, the particle size and bulk modulus of the reacting metal most probably influence the ignition time of MSRs. Namely, higher ductility (low bulk modulus) and finer particles seem to shorten the activation period before the MSR ignition. This study forms a cornerstone for further research in MSRs of metal chalcogenides because it universally assesses the influence of more parameters on the MSR course under fixed milling conditions for different systems. The proposed synthetic pathway also represents an improvement by reducing both time and energy by showing the possibility to reach some of the desired products within a minute-range, being much faster than a classical gradual reaction and further underlines the environmentally benign character of mechanochemistry.

Received 11th October 2023
Accepted 12th February 2024

DOI: 10.1039/d3mr00001j

rsc.li/RSCMechanochem

1. Introduction

Metal chalcogenides (MCs) are very promising materials for a rich plethora of applications, and the most studied ones include energy conversion (*e.g.* electrocatalysis,[1,2] batteries,[3] solar cells[4] or thermoelectrics[5]) and biological applications.[6] Their environmental applications[7] including photocatalysis[8] are also very beneficial. The recent focus of scientists is on preparing 2D,[9,10] 3D[11] and layer-structured anisotropic MCs[12] to further boost their application potential.

There are many synthetic pathways to obtain these compounds, which can be divided into wet chemical synthesis, high-temperature fabrication and chemical/physical deposition.[13] However, most of these methodologies bear the environmental burden, mostly by the necessity of utilizing multi-step methodologies, organic solvents, toxic organometallic precursors, and elevated temperature and pressure. These disadvantages can be overcome by utilizing mechanochemical synthesis, an alternative route to traditional chemistry.[14,15] In this case, the processes are performed solely in the solid state and the mechanical energy that is supplied to the treated powders *via* grinding causes the reactions to occur in a much simpler way. Its scalability potential is also interesting for industry.[16] This methodology is well-

[a]*Institute of Geotechnics, Slovak Academy of Sciences, Watsonova 45, 04001 Košice, Slovakia. E-mail: balazm@saske.sk*

[b]*Institute of Materials Research, Slovak Academy of Sciences, 04001 Košice, Slovakia*

[c]*Donát Bánki Faculty of Mechanical and Safety Engineering, Óbuda University, Népszínház utca 8, 1081 Budapest, Hungary*

† Electronic supplementary information (ESI) available. See DOI: https://doi.org/10.1039/d3mr00001j

established for the preparation of nanocrystalline metal chalcogenides.[17]

As precursors, often various compounds, such as salts can be used. For sulfides, in 2003, a so-called acetate route to produce various metal chalcogenides by using metal acetate and sodium sulfide as a source of metal and sulfur, respectively, was introduced.[18] However, the simplest way is to introduce elemental precursors. This was done many times in the past for a wide variety of MCs. Almost always, an argon protective atmosphere was used.

In mechanochemistry, the reactions can proceed in such a way that they take place in one moment (*i.e.* for a long time only the precursors can be identified and then suddenly in a very short timeframe, products are formed). Although such a pathway is clear from the results, the authors usually do not pay great attention to this, as mere information that the product was obtained is satisfactory for them. However, they are of great interest both from scientific and energy-saving points of view. These reactions are called mechanically induced self-propagating reactions (MSRs). A MSR is a reaction where the majority of the reagents instantly transform into products after a critical milling time (the ignition time which can also be in the range of seconds) through a combustion-like process, which is accompanied by a significant temperature and pressure increase.[19,20] This process is analogous to self-propagating high-temperature synthesis (SHS), where the self-propagating reaction is activated by supplying heat. The possibility to reach the products *via* a MSR brings about a reduction in both energy and time since it is usually much faster than the classical gradual reaction.

The occurrence of MSRs can be evidenced by using specially tuned grinding jars with gas temperature and/or pressure measuring availability,[21] or also by collecting characterization data directly during milling, *i.e. via in situ* monitoring of mechanochemical reactions (*e.g.* using XRD or Raman spectroscopy).[22–24] The former was recently accomplished for the Zn–S system.[25]

In relation to metal chalcogenide preparation, MSRs were reported for the first time already in 1982.[26] In this pioneering study, five metals (Cd, In, Pb, Sn and Zn) were reacted with chalcogens (S, Se and Te) and the MSR events were usually observed within tens of minutes or hours. Apart from this study, no systematic research considering the MSRs of more metal chalcogenides was reported. Detailed studies on MSRs are available for Zn–Sn–S/Se systems.[27–34] For other metal–chalcogen systems, the reports are less numerous. Namely, from the binary ones Cd–Se,[35] Cu–S,[36] Zr/Ti/Hf–S[37] and Fe/Ni_9S_8,[38] from ternary ones CuInS/Se_2 (ref. 39–41) and $MgCr_2S_4$ (ref. 42) and from quaternary ones Cu_2FeSnS_4 (ref. 43) systems can be mentioned.

The fundamental reports on what is actually governing the MSRs of MCs are scarce. In some studies, one system was investigated in detail and the effect of changing milling conditions on the MSR was studied (*e.g.*[31,44,45]). The other perspective, being the investigation of different systems under the same milling conditions, is rare, namely when the influence of various properties of the reagents and thermodynamics are considered. Some factors, including the thermodynamic ones, are tackled in the reviews by Takacs,[20,46] or more recently in the work of Ebrahimi-Kahrizsangi,[47,48] where the influence of melting temperature of reagents is investigated in detail. Particularly for MCs, Tschakarov has proposed that there is a clear relationship between hardness of the reagents and the ignition time.[26]

The aim of this study is to verify the results and hypotheses formulated by other researchers reported earlier on a set of MSRs to yield different metal sulfides and selenides. Specifically the influence of reagents melting temperature difference, bulk modulus of the used metals, ratio of enthalpy of formation of the products and heat capacity of the products and Gibbs free energy of formation of the products on the ignition time is investigated. Moreover, it also shows the possibility to prepare a bunch of nanocrystalline metal chalcogenides *via* the MSR pathway within a second or minute range in an air atmosphere. The MSR pathway for nickel-based systems is reported for the first time. The present work could bring renaissance for utilizing this type of reaction pathway to become widely applied for the preparation of materials based on metal chalcogenides.

2. Results and discussion

The influence of various factors governing mechanically induced self-propagating reactions is still poorly understood. To tackle this, we performed a universal study by igniting MSRs for a set of sulfides and selenides under the same milling conditions using six different metals (Cd, In, Pb, Sn, Ni and Zn) and two chalcogens (S and Se). Initially, it was necessary to characterize the precursors in terms of their particle size and morphology.

2.1. Particle size distribution and morphology of the precursors

To investigate the effect of the morphology and particle size of the precursors used in this study, SEM and laser diffraction, respectively, were employed (see Section S1 in ESI, S1†). Diverse morphology of the used metallic precursors can be seen from the SEM images in Fig. S1 and S2.† Zinc and cadmium particles were spherical, much finer in the former case. Lead and indium particles reminded spheres, but often irregularities and deformations were found. Nickel metallic powder consisted of very fine cubes and for tin, quite large platelet-like morphology was found. Regarding chalcogens, sulfur particles had a non-uniform shape, whereas selenium powder was composed of porous spherical particles, which were sometimes joined together.

The particle size distributions of the precursors are summarized in Fig. S3.† The size distribution is usually bimodal with d_{50} values in the range between 24 and 36 μm for three out of the six used metals. Nickel particles were much finer (unimodal size distribution with a d_{50} value below 7 μm) and on the other hand, those of tin and indium were quite large (with d_{50} values 80 and 89 μm, respectively). Chalcogen particles were finer than metallic ones (with the exception of Ni), sulfur being slightly finer.

2.2. Determining the ignition time of MSRs by gas pressure and temperature monitoring

In order to be able to evaluate the individual effects of different physico-chemical properties, it was necessary to determine the ignition time (t_{ig}) of MSRs, which is taken as a measure of the reactivity. The successful occurrence of MSRs can usually be identified already by human senses. The desired products usually have a different physical appearance than the reagents. Most often, the products are black, but *e.g.* ZnSe and CdS are orange. The powder after a successful MSR is usually covered on the milling balls and is stuck on the jar walls, and has the appearance of a sintered powder due to the heat that occurred during the event, far from being fine powder introduced into the milling chamber. Also the walls of the milling chamber are warmer than they would be in the case of simple milling without the occurrence of the MSR. In the moment of MSR occurrence, a specific smell of sulfur (rotten egg smell) or selenium (decayed horse-radish) can be detected sometimes. It is also evident after opening the chamber, when a small amount of smoke can be sometimes detected. We are of the opinion that this is the result of the interaction of chalcogenides with the atmospheric gases, rather than reaction gaseous by-products. In some cases, a small amount of powder is present on the lid on the top of the chamber. Specifically for some selenides, this powder was red. Its amount was too small to be analyzed *via* XRD. However, according to the literature, it will most probably be amorphous red selenium.[39] The photograph of the milling jar lid with this reddish powder after the preparation of one of the selenides is provided in the ESI (Fig. S4).† The MSR event was sometimes found to be accompanied by a scratching sound coming from the chamber. However, according to the empirical experience, it was not a general rule and in many cases, despite this sound could be heard, the MSR event did not occur yet. In general, the examination using senses is of course not satisfactory for the precise determination of the ignition time. Therefore, we performed the high-energy ball milling experiments in a special milling chamber equipped with a sensor for measuring the pressure (p) and temperature (T) of the gas inside. In this way, the changes in p and T can be continuously monitored during milling and any abrupt pressure and/or temperature change, documenting the occurrence of a MSR, can be well seen.

In Fig. 1a and b, the changes in gas pressure (representative curves) for the synthesis of sulfides and selenides performed at 750 and 400 rpm, respectively, are shown. The reason for performing the reactions to yield selenides at a lower milling speed is their much higher reactivity in comparison with sulfides, and thus the inability to clearly observe the MSR ignition. More details are provided in the Section S2 in the ESI, including Fig. S5–S11.† Together with pressure monitoring, also the temperature was monitored, but the MSR event could not be determined in this way (no abrupt increase can be observed in Fig. S12†), due to the limitations of the experimental setup.[21]

As a representative parameter indicating the start of the process, the ignition time (t_{ig}) determined by the onset of the sharp pressure increase was considered. The pressure increase and decrease usually take place within 5 seconds and as the equipment records the pressure changes only each two seconds, it cannot be claimed that the evidenced pressure value is the maximum pressure achieved during the MSR. This was proven by comparing the different values of maximum pressures for the repeated experiments where significant differences were observed. It is also possible that in the case of small pressure increase, the event can also be completely missed. Therefore, we consider only t_{ig} as a measure of MSR occurrence in this study and this approach is in accordance with other studies.[28,31]

In five out of the six studied sulfides and selenides, an abrupt pressure increase and decrease after a short activation occurred, which is a proof of the MSR event.[36] In the case of tin sulfide and indium selenides, the MSR event was not observed. According to (ref. 49), for the SnS synthesis to run through the MSR pathway, it is necessary that the tin : sulfur molar ratio is at least 0.9. This condition is fulfilled in our case. Together with the Zn–S system, this system has been well-researched in the literature, however, the reasons why this reaction should not exhibit the MSR pathway in our case remain unclear. Similarly, the absence of the MSR pathway for the In–Se mixture, which is in contradiction with the pioneering work,[26] remains a mystery. In contrast to the Sn–S system, there is a lack of relevant literature available for the In–Se system. One of the hypotheses could be

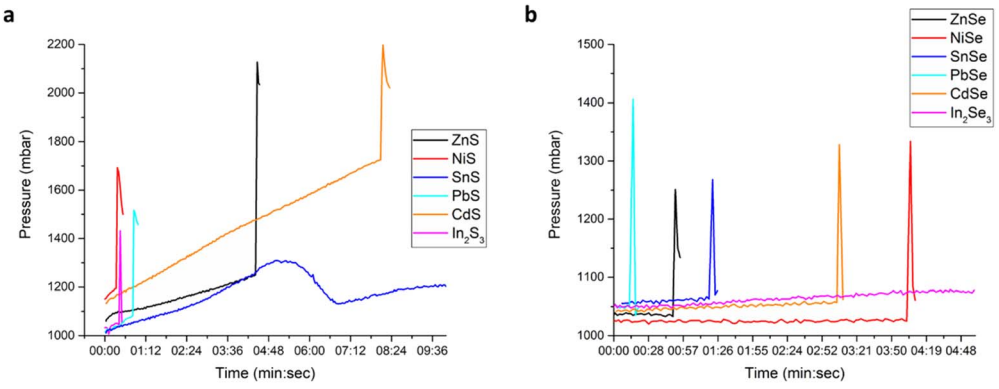

Fig. 1 Gas pressure changes during milling (representative curves): (a) Me–S mixtures treated at 750 rpm and (b) Me–Se mixtures treated at 400 rpm.

the low bulk modulus of the metals in question; however, as will be shown later (Section 2.3.4), the other metals with quite similar bulk moduli reacted *via* the MSR pathway and even In and Sn reacted with S and Se, respectively, *via* a MSR pathway. Indeed, the low bulk modulus seems to be beneficial for MSR ignition. It is probable that upon properly tuning the properties of the starting powders and milling conditions, the MSR events should occur also in these two cases, but this is beyond the scope of this study.

Apparently, the formation of selenides is more feasible than that of sulfides, as with the exception of Ni-based systems, the MSR events occur sooner than for sulfides, which is in accordance with ref. 26. Despite the fact that milling of Me–Se systems was conducted at a lower milling speed (400 rpm), the reactions were still faster. The ignition time increases for the synthesis of both sulfides and selenides in the following order: Pb < Zn < Cd, in alignment with ref. 26. Ni-based systems are an exception and require further research. The ignition times of each reaction mixture where the MSR was observed are provided in Fig. 2.

As our study was strongly based on the pioneering one by Tschakarov *et al.*,[26] we tried to provide some direct correlations with that report. In 1982 when that study was published, the available mechanochemical equipment was not able to supply as much energy as it does nowadays, namely, the authors used a low-energy vibratory mill, being compeltely different from the planetary ball mill used in the present study. Therefore, the ignition times were by far longer there. Firstly, we have plotted the ignition times described in that study together with ours (Fig. S13a†). It can be seen that the trend is quite similar for four elements, albeit the synthesis of Zn-based systems was faster and that of Cd-based ones was slower in our case. If the t_{ig} values reported in (ref. 26) (in seconds) are divided by ours, we get the information about how many times the reactions were faster in our case. This information is plotted in Fig. S13b.† Except Zn- and Cd-based systems, all the reactions were in the range from 25 to 60 times faster in our case. The reactions of Zn with S and Se were 104 and 374 times faster, respectively, whereas those of Cd were only 9 and 15 times faster, respectively. These discrepancies detected for Zn- and Cd-based systems most probably deal with the specification of the used precursors.

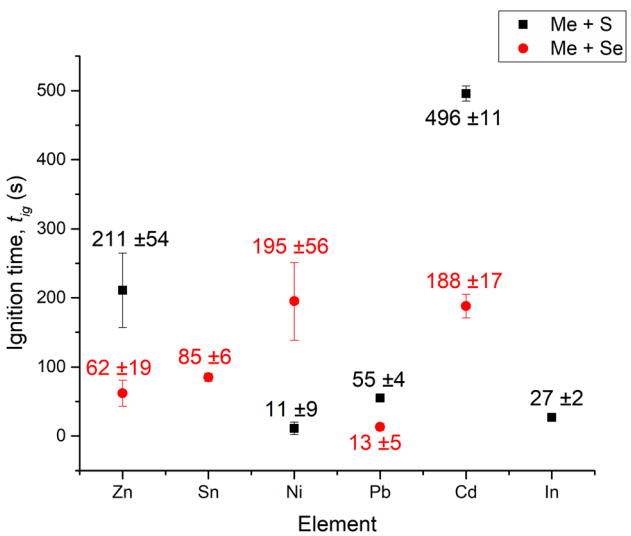

Fig. 2 Ignition times (t_{ig}) of the investigated Me + S and Me + Se MSRs.

2.3. Considerations about the influence of various properties of the reagents on the ignition time

2.3.1. Particle size of the reagents. The dependence of ignition time (t_{ig}) on the median particle size of the metallic precursors (d_{50} obtained from the measurements shown in Fig. S3†) for both Me–S and Me–Se systems is shown in Fig. 3a. Clearly, no relationship between d_{50} and t_{ig} could be found for neither sulfides or selenides. Obviously, the used materials are completely different from the chemical point of view and also other properties than particle size are important. In Fig. 3a, the fact that we are dealing with different metals is completely neglected. However, we are of the opinion that if one reaction system would be investigated, decreasing the particle size of the precursors would have a positive impact on the ignition time. We are not aware of any systematic study that would tackle this issue for MSRs; however, there are reports on self-propagation high-temperature synthesis (SHS), an analogous combustion-like process ignited by heating, not by high-energy ball milling. Namely, when the particle size of carbon was ~1 μm, the SHS in the Ni–Ti–C system was ignited after ~9000 ms, and the temperature increased from room temperature to 2567 K immediately, whereas when the particle size of carbon was 38 and 75 μm, the reaction occurred after 30 000 and 40 000 ms, respectively, and the temperature was increasing for around ~20 000 s in both cases.[50] In another study, the effect of Mg (used as a reducing agent) particle size on the SHS of the B_4C–TiB_2 system was investigated.[51] Upon decreasing the Mg particle size, the amount of residual Mg decreased; however, no information about the impact on t_{ig} is provided. We are of the opinion that particle size reduction was also the key point why the MSR could be ignited immediately in the case of Cd + Se and Zn + Se mixtures after the prior mechanical activation of the two reagents in ref. 35. It seems that bringing down the particle size below a certain critical value could ignite MSRs even in the cases where it was never observed before (like shown for a Cu–S system by our research group in 2016 (ref. 36) or for Ni–S and Ni–Se systems shown for the first time in this study; in both these cases, the particles were very fine). This creates a great field for future research.

However, let's imagine a very simplified situation that all the metallic precursors have the same mean particle size of 25 μm and all the particles are perfectly spherical. Let's also imagine that there is a linear relationship between the particle size of the given metal and the ignition time that is necessary for the MSR between this metal and chalcogen to occur. Under these circumstances, we can re-calculate the t_{ig} data from Fig. 2. Namely, t_{ig} for the metals where d_{50} values were larger than 25 μm will be shorter and for the finer powders, it will be proportionally longer. The re-calculated ignition times $t_{ig\text{-}25}$ (together

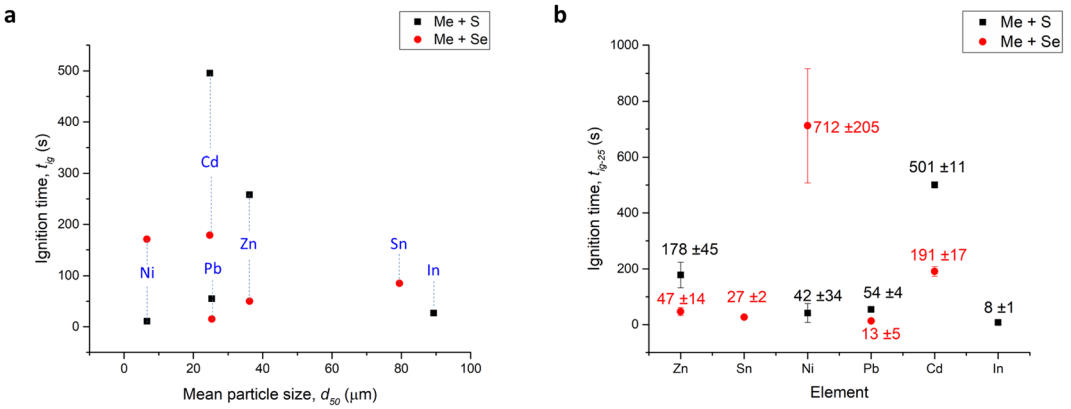

Fig. 3 (a) The dependence of t_{ig} of MSRs to yield sulfides (S) and selenides (Se) on d_{50} values and (b) re-calculated ignition time neglecting the influence of particle size and morphology (t_{ig-25}).

with proportionally re-calculated standard deviations) are shown in Fig. 3b. In this situation, we completely neglect the influence of particle size and morphology and ascribe all the difference in t_{ig} just to the different properties of the elemental precursors that will be discussed below. For this reason, we are using the dependence of t_{ig-25} on these properties in further text. We are of course aware that this is over-simplification, but it can provide at least an estimation on the influence of the other physico-chemical properties and moreover, this estimation does not dramatically change the trend observed in Fig. 2.

2.3.2. Hardness of the reagents. Tschakarov *et al.* have reported a clear relationship between the microhardness of elements and t_{ig}. Therefore, we plotted t_{ig-25} against hardness in Fig. 4a (for comparison also the data from the pioneering study[26] are shown in Fig. 4b).

The apparently linear relationship in the case of ref. 26 presented in Fig. 4b cannot be overlooked; however, the results are not perfect and clearly the deviations from the trend can be identified (*e.g.* the t_{ig} for Sn which is softer than In was longer). According to the suggestion of the authors, the softer the metal and the harder the chalcogen, the sooner the MSR event occurs.[26] In our case, no clear relationship could be found (Fig. 4a), so it seems that it is not possible to ascribe the resulting ignition time only to the hardness of the metal. We also tried to find some information about the relationship between the hardness of the metals and the course of SHS they take place in, but it was not possible to find any relevant information, unlike the relationship with particle size.

2.3.3. Melting temperature of the reagents. About a decade ago, a relationship to describe the dependence of the ignition time on the reagent melting temperature (T_m) was proposed.[47,48] Namely, the model suggests that the t_{ig} increases with the arithmetic mean of the T_m of the reagents. The process was investigated for many inorganic reaction mixtures in the mentioned study using experimental data from the literature; however, chalcogenides were not analysed. We were curious whether similar or at least some relationship can be found in our systems (Fig. 5a). The obtained results were surprising. There seems to be a maximum of t_{ig} reached at around the T_m arithmetic mean around 250 °C and both below and above this value, the t_{ig} values decrease in an exponential manner. To the left part from this maximum, the points obtained for Me + S

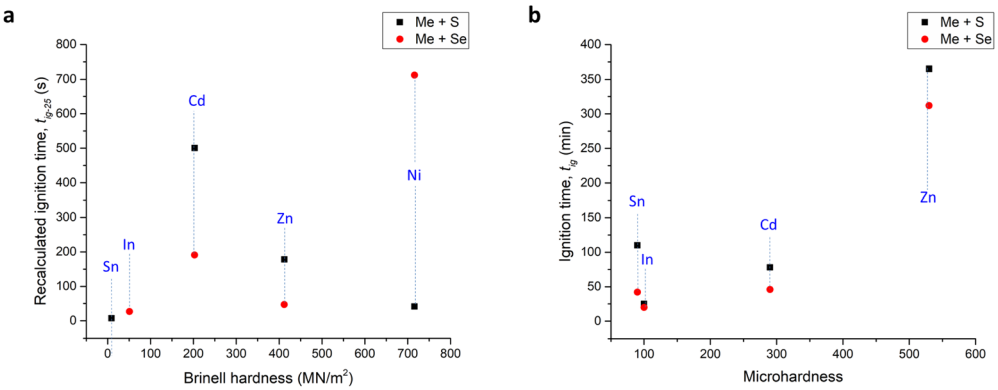

Fig. 4 Influence of hardness on the time of ignition: (a) data from this study and (b) data from (ref. 26). By *T*, the results from the study[26] are labeled. The hardness source data in our study were taken from ref. 52 and in ref. 26, it was from ref. 53 and although different types of hardness are plotted (Brinell hardness *vs.* microhardness), the relative differences between the metals are the same in both sources. For lead, hardness data were not available in neither of the studies.

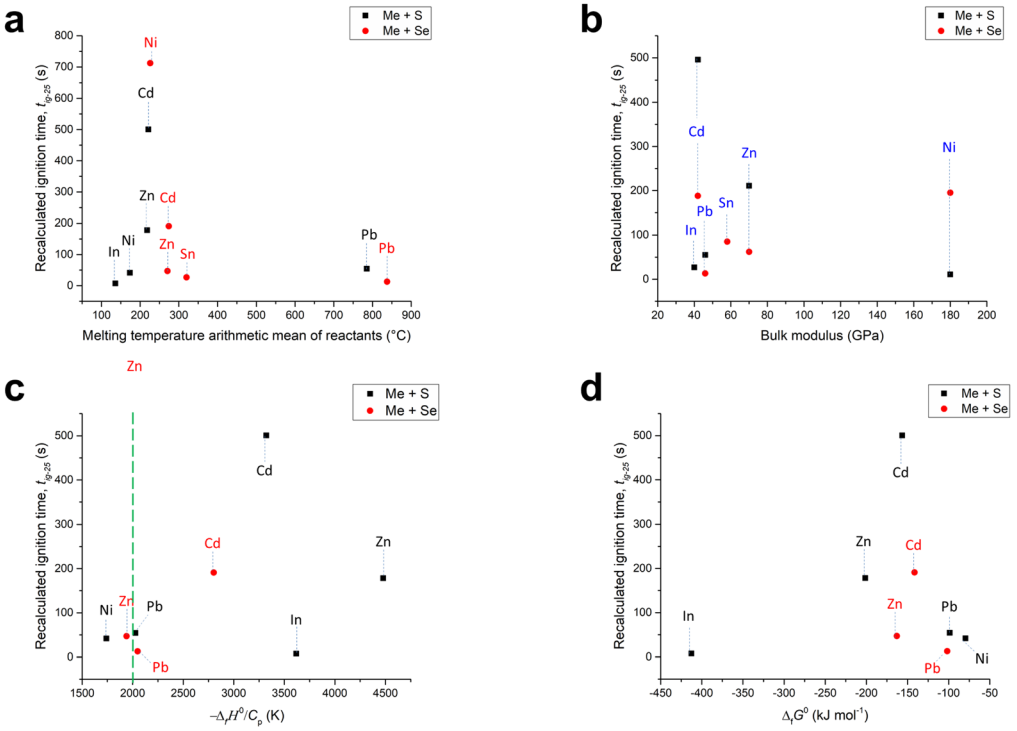

Fig. 5 The dependence of recalculated ignition time (t_{ig-25}) on: (a) the arithmetic mean of melting temperatures of the reagents, (b) bulk modulus, (c) ratio between standard enthalpy of formation and heat capacity of the product; green line represents the generally accepted borderline between the MSR region to the right and non-MSR one to the left, and (d) standard Gibbs energy of formation of the product. Source data are taken from ref. 52 and 56–62. For tin and nickel selenides, information about the bulk modulus and ΔG could not be found.

systems and to the right, those obtained for Me + Se systems are located. The points for Pb-containing systems are not in this region, as the T_m arithmetic mean of the reagents is much higher in this case (namely 785 °C for Pb + S and 838 °C for Pb + Se). Despite the large difference in T_m, the t_{ig} is quite short. Thus, the increase of t_{ig} with the arithmetic mean of T_m of the reagents reported in ref. 47 and 48 was evidenced only for Me + S systems and at quite low temperatures, and for Me + Se systems, an opposite trend was observed. The obtained results are peculiar, but it would be too bold to say that the observed relationship is fully justified and providing any explanations at this point would be pure speculations. Nevertheless, it surely brings in a new perspective for future research. Moreover, it has to be kept in mind that the melting temperature decreases with decreasing particle size.[54] This accounts also for metals,[55] and this behavior is explained by the Gibbs–Thomson equation. This means that if the size of precursors drops below a certain value during the activation phase preceding the MSR, the melting could occur at much lower temperatures than generally valid for those substances. Nevertheless, according to the XRD patterns recorded shortly before MSRs for many systems in the literature (*e.g.* (ref. 25, 35 and 44)), the diffractions of the precursors are still quite strong and sharp, which documents that the precursor particles are not too fine when entering the MSR and the melting temperature is most probably not affected to a large extent.

2.3.4. Bulk modulus of the reagents. Another important mechanical property of the metals is the bulk modulus, *i.e.* their incompressibility. The relationship between the bulk modulus of the metals used in this study and MSR ignition time of Me + S, or Me + Se systems is given in Fig. 5b. Different behaviors of Cd and Ni-based systems do not fall into the trend here, but for In, Pb and Zn, a quite nice relationship could be found in the case of sulfides. For selenides, Zn does not fit into the trend and potentially, an opposite linear relationship in Cd, Sn and Zn selenides can be seen; however, we are of the opinion that this is caused by the lower reactivity of Cd rather than a genuine reason. In general, with increasing the bulk modulus of the metal, the occurrence of the MSR seems to be delayed. Thus, the more refractory character of the metal seems to be detrimental for MSR occurrence. Here, a parallel with the claims made regarding hardness in the pioneering work can be traced,[26] *i.e.* the softer the metal, the quicker the MSR. According to Avvakumov and Kosova,[63] the higher ductility (*i.e.* lower bulk modulus) increases the formation of interfaces between the component particles. This would be in accordance with the looming trend visible for sulfides, *i.e.* the more ductile the metal (*i.e.* having a lower bulk modulus), the earlier the MSR occurs.

2.3.5. Ratio of enthalpy of formation and heat capacity of the products, $\Delta H/C_p$. The thermodynamic constants might be also of some help in understanding the course of MSRs. For a long time, an accepted rule of thumb was that for the reaction to potentially take place as a MSR, the ratio of enthalpy of

formation and heat capacity of the product ($\Delta H/C_p$) has to be higher than 2000 K.[20,64] For our studied systems, this condition is accepted for the majority; however, the $\Delta H/C_p$ ratio is slightly lower for ZnSe and well-below this threshold for NiS and despite this, the MSR was observed. It is also well below the threshold for the CuS formation (this ratio is 1039 K) and we could observe the MSR for this system previously.[36] Thus, it seems that $\Delta H/C_p$ equal to 2000 K is not a limiting factor for the MSR to occur and it is possible to ignite MSRs for the systems not respecting this. In order to investigate whether there is any relationship between the $\Delta H/C_p$ ratio and ignition time, the plot in Fig. 5c was elaborated. No correlation could be found, being in accordance with the data from the pioneering work[26] and for the one introducing the reagents melting temperature difference theory.[47,48] Takacs in his review also mentions that in most cases, little connection is found between the ignition time and $\Delta H/C_p$ and supports the theory that the mechanical properties are important,[46] which is in alignment with trends observed for the bulk modulus in Fig. 5b. However, there is an example where $\Delta H/C_p$ could be well-correlated with t_{ig}, namely for the reduction of some metal oxides with Ti, Zr and Hf.[37,65]

2.3.6. Gibbs energy. The free Gibbs energy of formation is another important thermodynamic parameter and we tried to find whether there is any correlation between ΔG and $t_{ig\text{-}25}$ (Fig. 5d). We did not detect any sensible correlation, as in the case of Me + S systems, with decreasing ΔG, there is at first increase and then decrease of t_{ig}. Regarding selenides, no conclusion can be made based on three points. For comparison, we plotted also the data from the pioneering study[26] in the ESI (Fig. S14†), which showed that the higher the ΔG, the slower the process. Mechanochemistry is known not to respect thermodynamic rules[66,67] and the processes can be rather governed by the activation energy that influences the kinetics. On the other hand, also the study showing the opposite results was published,[48] namely the ignition time was decreasing with the increasing enthalpy of formation ΔH, the values of which are usually very close to ΔG. However, this was studied for the single system (B_2O_3–TiO_2–Al) where the thermodynamic changes were measured.

2.3.7. General viewpoint. We discussed only a fraction of possible properties that could be important for the course of MSRs here. There seems to be some correlation between mechanical properties and ignition time (Fig. 5b), however, for the rest of the investigated properties and thermodynamic parameters, no solid conclusion could be drawn. It seems that each system can have its own characteristics, and it is necessary to examine in detail each of them. Moreover, it seems that any prerequisites that are predetermining whether or not the MSR will run and how long it will take until ignition can be forgotten if the particle size of the reagents is sufficiently small. As discovered in 2016 for copper sulfides by our group,[36] the fine Cu particles with needle-like morphology reacted with sulfur *via* the MSR pathway, whereas the atomized powder ones with spherical morphology did not. We have shown the MSR event for the nickel chalcogenides here, and, as was discussed above, according to the theory, the exothermicity of this reaction should not be high enough to be susceptible to MSRs. Despite this fact, it occurred, and also in this case, nickel particles were very fine. Very fine powder can be also obtained *via* pre-milling. This was shown in the case of the Cd–Se system in the past,[35] where the ignition time could be reduced from 120 s to less than 5 s by pre-activating the precursors. This pre-activation has definitely influenced the particle size and smaller particles are more prone to react faster. We therefore suggest and plan for the future a detailed investigation on the effect of particle size for the selected system on the ignition time, as for now, it is the only parameter that undoubtedly shows a strong influence on the MSR onset.

2.4. Determination of the phase composition *via* X-ray diffraction

The successful formation of the desired products in a short time after the MSR event can be well-traced by X-ray diffraction. The XRD patterns are provided in Fig. 6. Each XRD pattern is plotted also individually with the corresponding bar graphs of the identified crystallographic phases from the ICDD-PDF2 database in the ESI (Section S4, S5 and Fig. S15–S26).† To estimate the crystallite size of the desired metal chalcogenide and also the amount of unreacted metal, the Rietveld refinement of the XRD patterns of the selected samples was performed and the results are also provided in Fig. 6. The Rietveld plots are provided in the ESI in Fig. S15–17 and S21–25† as part "b".

The obtained XRD patterns can be divided into three groups. The first group contains high-intensity peaks of the desired products with a small amount of unreacted metals (this is valid for all patterns in Fig. 6a and c, and for Ni–Se and Sn–Se systems shown in Fig. 6d). In these cases, the MSR event was observed and clearly led to the formation of the desired compounds and also the Rietveld refinement of XRD data was feasible. The presence of a small amount of residual unreacted metal is in accordance with the results reported for Zn–S mixtures in the past,[25,31] or also for the Cd–Se system.[35] It is most probably connected with the volatility of chalcogens during the MSR event, which remains attached to the jar lid after the event, where the reacting powder does not have access. This is also supported by the presence of red powder found on the lid in few reactions of the Me–Se system (Fig. S4†), which might potentially be red selenium. In order not to observe residual elements, the reactions could be potentially run with slight over-stoichiometry of chalcogens. The sharp diffraction peaks of the main products hint at their good crystallinity, which is in contrast with traditional gradual mechanochemical reactions, which usually yield nanoparticles with size below 20 nm and broad peaks in the XRD patterns.

The second group of XRD patterns is represented by the mixtures, where the MSR event was observed *via* a GTM device, and the consumption of the majority of reagents can be confirmed *via* XRD; however, the final product is composed of a mixture of various phases of the particular metal-chalcogenide system. This accounts for Ni–S and In–S XRD patterns in Fig. 6b.

The last third group is represented by two XRD patterns for Sn–S (in Fig. 6b and S19†) and In–Se (in Fig. 6d and S26†), where

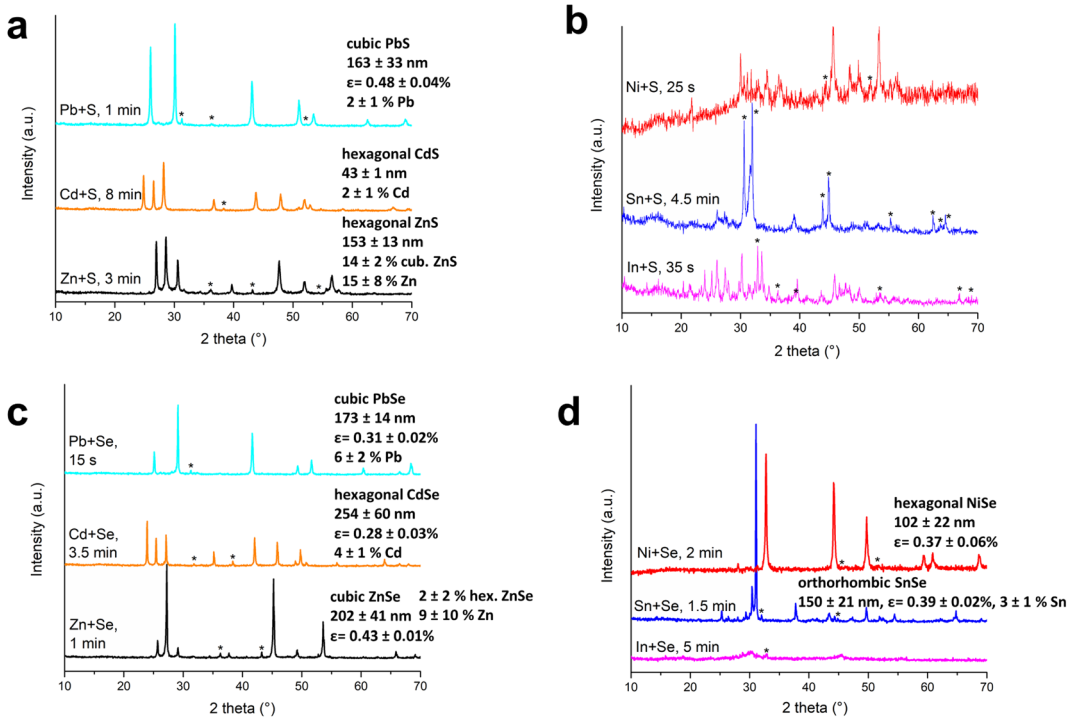

Fig. 6 XRD patterns of the sulfides synthesized at 750 rpm (a and b) and selenides synthesized at 400 rpm (c and d) *via* a MSR pathway in this study. Milling time, crystallite size and microstrain (ε) of the produced chalcogenide estimated by Rietveld refinement is provided in the figure. ε did not seem to contribute to peak broadening for CdS and ZnS. The diffractions corresponding to unreacted metallic precursors are marked with an asterisk. All the unmarked diffractions belong to the prepared sulfide/selenide. Note: tin sulfide and indium selenide synthesis does not run *via* the MSR pathway under the studied conditions.

the MSR event did not take place. The XRD pattern of the Sn–S mixture taken after 4 min and 30 s of the treatment (Fig. 6b, blue pattern) exhibits the diffractions of both tin and SnS, which hints at the gradual reaction pathway. Similarly, the XRD pattern of the 2In + 3Se system after 5 min of milling shows the combination of both reagents and products, thus pointing to a gradual pathway. In this case, the XRD measurement was performed also on a different device with a better signal-to-noise ratio that showed a significant amount of elemental indium present (Fig. S26b†). The diffraction peaks of the detected indium selenides are very broad, thus pointing to very fine nanocrystals.

It has to be noted that also for the systems that we report the MSR to occur, it was not always the case upon numerous repetitions of experiments (albeit in most cases yes), despite performing the reactions under the same conditions. This occurred in two out of four trials to reach for NiS at 750 rpm and once when preparing SnSe and PbSe. The XRD patterns of these powders are provided in Section S6 of the ESI, namely in Fig. S27–S29.† In the case of NiS synthesis, a considerable amount of unreacted nickel and sulfur was observed after 2 minutes of the treatment (Fig. S27†); however, if the MSR pathway is followed, the XRD pattern is free from precursors in 25 seconds (Fig. 6b and S18†). Regarding the Sn–Se system, the XRD pattern of the product not formed *via* the MSR measured after 5 minutes of treatment at 400 rpm shows the presence of a higher amount of unreacted tin (Fig. S28†) in comparison with the product after the MSR (Fig. 6d and S25†), which took place after 90 seconds. This XRD pattern is very similar to the one obtained after the MSR event at 750 rpm (Fig. S8†). This result provides another proof of the high impact of changing rotation speed on the outcome of the MSR. In the case of PbSe, the milling was conducted for 3 minutes and no traces of elemental lead can be seen in the XRD pattern (Fig. S29†). In this case, it is possible that the reaction was already completed in a gradual regime. In, general, the reasons why the MSR sometimes does not occur under the identical conditions for the same system are not clear for now and will be a subject of future research. There might be some minor peculiarities that we have missed in the present research.

3. Materials and methods

3.1. Materials

The starting materials of the present research encompassed nickel (Penta, Czech Republic), copper (electrolytic, Pometon, Germany), zinc (Merck, Germany), lead (ITES, Slovakia), cadmium (Alfa Aesar, Germany), tin (Merck, Germany), sulfur (Ites, Slovakia) and selenium (Merck, Germany) and were used as-received from the providers without subsequent purification. The information about particle size distribution and morphology of the precursors is provided in the paper.

3.2. Mechanochemical synthesis

The mechanochemical synthesis was performed in a Pulverisette 7 Premium line planetary ball mill (Fritsch, Germany)

under the following conditions: overall sample mass 5 grams, air atmosphere, 24 tungsten carbide (WC) milling balls with 10 mm diameter weighing 180 g, WC milling chamber with 80 mL diameter, ball-to-powder ratio 36, and milling speed 400 or 750 rpm. The masses of individual elements were calculated to reach the desired stoichiometry Me_xS/Se_y, where x and $y = 1$ (In-based systems were an exception, here $x = 2$ and $y = 3$). In order to investigate the pressure and temperature of the gas during milling, milling was performed in a special milling chamber equipped with the corresponding sensors, namely *via* using an Easy GTM system (Fritsch, Germany). The obtained data were recorded *via* MillControl software (Fritsch, Germany). Each experiment was performed at least two times. Milling was stopped as soon as possible after the occurrence of the MSR event, which always took place within 10 minutes of the treatment.

3.3. Characterization

The identification of phase composition was performed by X-ray diffraction with a D8 Advance diffractometer (Bruker Germany) using Cu Kα (40 kV, 40 mA) radiation. The patterns were recorded in the 2 theta range 15–80° using a step time 10 s and step size 0.03°. The refinement was performed using TOPAS_Academic software.[68,69] The selected XRD patterns were recorded using an X'Pert Pro (Philips) diffractometer equipped with Cu Kα radiation, operating at 40 kV and 50 mA in the 2 theta range between 10 and 70° and using a time per step of 30 s and step size of 0.033°.

The grain size analysis of the precursors was performed using a particle size laser diffraction analyzer Mastersizer 2000E (Malvern Panalytical, Malvern, UK) in the dry mode. Each sample was measured three times.

The morphology of the precursors was investigated with a scanning electron microscope Tescan Vega 3 LMU (TESCAN, Brno, Czech Republic) using an accelerating voltage of 20 kV. In order for the samples to be conductive, the powder was covered with a layer of gold on a FINE COAT ION SPUTTER JFC-1100 fy (JEOL, Akishima, Japan). To obtain information about chemical composition, an energy-dispersive X-ray spectroscopy (EDS) analyzer Tescan: Bruker XFlash Detector 410-M (TESCAN, Brno, Czech Republic) was used. The same device was used to record elemental maps.

4. Conclusions

The present study aimed to bring renaissance to the systematic research field of mechanically induced self-propagating reactions by showing them to be a powerful tool to prepare nanocrystalline metal chalcogenides with great application potential in an energy-efficient and environmentally benign manner. Namely, the reactions of Cd, In, Ni, Pb, Sn and Zn with S and Se were investigated. Most of the desired compounds could be prepared within the second-range, maximum up to 9 minutes. For 10 out of 12 studied metal chalcogenide systems, the MSR event was successfully confirmed *in situ via* an abrupt gas pressure increase inside the milling jar and subsequently *via* X-ray diffraction. Selenides were proven to be formed much faster than sulfides, and thus the milling speed needed to be decreased from 750 rpm to 400 rpm to be able to trace down the process in this case. The hypothesis that solely hardness of the reagents is a key factor influencing the ignition time of the MSR was proven to be wrong. On the other hand, the particle size of the reagents and the bulk modulus of the reacting metals seem to influence the ignition time of the MSR. It seems that the finer the powder and the lower the bulk modulus of the reacting metal, the sooner the MSR occurs. Nevertheless, many questions remain unanswered, which leaves the door open for a further systematic research in this field.

Data availability

The datasets generated during and/or analysed during the current study are available from the corresponding author on reasonable request.

Author contributions

Conceptualization: M. B.; methodology: M. B. and T. C.; software: M. B.; validation: M. B., R. D., R. B., T. S. and T. C.; investigation: M. B., R. D., R. B., T. S. and T. C.; resources: M. B.; data curation: M. B., R. D., R. B., and T. S.; writing – original draft preparation: M. B.; writing – review and editing: M. B., R. D., R. B., T. S. and T. C.; visualization: M. B.; supervision: M. B.; project administration: M. B.; funding acquisition: M. B. All authors have read and agreed to the published version of the manuscript.

Conflicts of interest

The author(s) declare no competing interests.

Acknowledgements

This work was supported by the Slovak Research and Development Agency under the contract No. APVV-18-0357 and by the Slovak Grant Agency VEGA (project 2/0112/22 and 2/0084/23). The support of COST Action CA18112 MechSustInd (**https://www.mechsustind.eu/**), supported by the COST Association (European Cooperation in Science and Technology, **https://www.cost.eu/**), is also acknowledged. This research has been also funded by the Committee of Science of the Ministry of Education and Science of the Republic of Kazakhstan (Grant No. AP14870472). T. C. is grateful for the funding of the Slovak Academy of Sciences *via* the project of Seal of Excellence H2020-MSCA-IF (Strengthecs).

References

1 M. R. Gao, Y. F. Xu, J. Jiang and S. H. Yu, Nanostructured metal chalcogenides: synthesis, modification, and applications in energy conversion and storage devices, *Chem. Soc. Rev.*, 2013, **42**(7), 2986–3017.

2 M. Shao, Q. Chang, J. P. Dodelet and R. Chenitz, Recent Advances in Electrocatalysts for Oxygen Reduction Reaction, *Chem. Rev.*, 2016, **116**(6), 3594–3657.
3 H. Tan, Y. Feng, X. Rui, Y. Yu and S. Huang, Metal Chalcogenides: Paving the Way for High-Performance Sodium/Potassium-Ion Batteries, *Small Methods*, 2020, **4**(1), 1900563.
4 K. Meng, G. Chen and K. R. Thampi, Metal chalcogenides as counter electrode materials in quantum dot sensitized solar cells: A perspective, *J. Mater. Chem. A*, 2015, **3**(46), 23074–23089.
5 C. Han, Q. Sun, Z. Li and S. X. Dou, Thermoelectric Enhancement of Different Kinds of Metal Chalcogenides, *Adv. Energy Mater.*, 2016, **6**(15), 1600498.
6 V. Agarwal and K. Chatterjee, Recent advances in the field of transition metal dichalcogenides for biomedical applications, *Nanoscale*, 2018, **10**(35), 16365–16397.
7 E. C. Okpara, O. C. Olatunde, O. B. Wojuola and D. C. Onwudiwe, Applications of Transition Metal Oxides and Chalcogenides and their Composites in Water Treatment: a review, *Environ. Adv.*, 2023, **11**, 100341.
8 T. S. Munonde and P. N. Nomngongo, Review on Metal Chalcogenides and Metal Chalcogenide-Based Nanocomposites in Photocatalytic Applications, *Chem. Afr.*, 2023, **6**(3), 1127–1143.
9 K. Pramoda and C. N. R. Rao, 2D transition metal-based phospho-chalcogenides and their applications in photocatalytic and electrocatalytic hydrogen evolution reactions, *J. Mater. Chem. A*, 2023, **11**(32), 16933–16962.
10 Y. Xiao, C. Y. Xiong, M. M. Chen, S. F. Wang, L. Fu and X. H. Zhang, Structure modulation of two-dimensional transition metal chalcogenides: recent advances in methodology, mechanism and applications, *Chem. Soc. Rev.*, 2023, **52**(4), 1215–1272.
11 H. Chen, M. Y. Ran, W. B. Wei, X. T. Wu, H. Lin and Q. L. Zhu, A comprehensive review on metal chalcogenides with three-dimensional frameworks for infrared nonlinear optical applications, *Coord. Chem. Rev.*, 2022, 470.
12 A. Giri, G. Park and U. Jeong, Layer-Structured Anisotropic Metal Chalcogenides: Recent Advances in Synthesis, Modulation, and Applications, *Chem. Rev.*, 2023, **123**(7), 3329–3442.
13 M. Channegowda, R. Mulla, Y. Nagaraj, S. Lokesh, S. Nayak, S. Mudhulu, C. K. Rastogi, C. W. Dunnill, H. K. Rajan and A. Khosla, Comprehensive Insights into Synthesis, Structural Features, and Thermoelectric Properties of High-Performance Inorganic Chalcogenide Nanomaterials for Conversion of Waste Heat to Electricity, *ACS Appl. Energy Mater.*, 2022, **5**(7), 7913–7943.
14 X. Liu, Y. Li, L. K. Zeng, X. Li, N. Chen, S. B. Bai, H. He, Q. Wang and C. Zhang, A Review on Mechanochemistry: Approaching Advanced Energy Materials with Greener Force, *Adv. Mater.*, 2022, **34**(46), 2108327.
15 F. Cuccu, L. De Luca, F. Delogu, E. Colacino, N. Solin, R. Mocci and A. Porcheddu, Mechanochemistry: New Tools to Navigate the Uncharted Territory of "Impossible" Reactions, *ChemSusChem*, 2022, **15**(17), e202200362.
16 E. Colacino, V. Isoni, D. Crawford and F. García, Upscaling Mechanochemistry: Challenges and Opportunities for Sustainable Industry, *Trends Chem.*, 2021, **3**(5), 335–339.
17 P. Baláž, M. Baláž, M. Achimovičová, Z. Bujňáková and E. Dutková, Chalcogenide mechanochemistry in materials science: insight into synthesis and applications (a review), *J. Mater. Sci.*, 2017, **52**, 11851–11890.
18 P. Baláž, E. Boldizarova, E. Godocikova and J. Briacin, Mechanochemical route for sulphide nanoparticles preparation, *Mater. Lett.*, 2003, **57**(9–10), 1585–1589.
19 P. Baláž, M. Achimovičová, M. Baláž, P. Billik, Z. Cherkezova-Zheleva, J. M. Criado, F. Delogu, E. Dutková, E. Gaffet, F. J. Gotor, R. Kumar, I. Mitov, T. Rojac, M. Senna, A. Streletskii and K. Wieczorek-Ciurowa, Hallmarks of mechanochemistry: from nanoparticles to technology, *Chem. Soc. Rev.*, 2013, **42**(18), 7571–7637.
20 L. Takacs, Self-sustaining reactions induced by ball milling, *Prog. Mater. Sci.*, 2002, **47**(4), 355–414.
21 R. Scholl, R. Wegerle and W. Mutter, Gas pressure and temperature measuring system (GTM) for in-situ data acquisition during planetary ball milling, *J. Metastable Nanocryst. Mater.*, 2000, **8**, 964–972.
22 A. A. L. Michalchuk and F. Emmerling, Time-Resolved *In Situ* Monitoring of Mechanochemical Reactions, *Angew. Chem., Int. Ed.*, 2022, **61**(21), e202117270.
23 A. D. Katsenis, A. Puskaric, V. Strukil, C. Mottillo, P. A. Julien, K. Uzarevic, M. H. Pham, T. O. Do, S. A. J. Kimber, P. Lazic, O. Magdysyuk, R. E. Dinnebier, I. Halasz and T. Friscic, In situ X-ray diffraction monitoring of a mechanochemical reaction reveals a unique topology metal-organic framework, *Nat. Commun.*, 2015, **6**, 6662.
24 S. Lukin, K. Užarević and I. Halasz, Raman spectroscopy for real-time and *in situ* monitoring of mechanochemical milling reactions, *Nat. Protoc.*, 2021, **16**(7), 3492–3521.
25 H. Petersen, S. Reichle, S. Leiting, P. Losch, W. Kersten, T. Rathmann, J. Tseng, M. Etter, W. Schmidt and C. Weidenthaler, In Situ Synchrotron X-ray Diffraction Studies of the Mechanochemical Synthesis of ZnS from its Elements, *Chem.–Eur. J.*, 2021, **27**(49), 12558.
26 C. G. Tschakarov, G. G. Gospodinov and Z. Bontschev, The mechanism of the mechanochemical synthesis of inorganic compounds, *J. Solid State Chem.*, 1982, **41**(3), 244–252.
27 V. Rusanov and C. Chakurov, Percolation phenomena in explosive mechanochemical synthesis of some metal chalcogenides, *J. Solid State Chem.*, 1990, **89**(1), 1–9.
28 L. Takacs, Self-sustaining metal-sulfur reactions induced by ball milling, *J. Mater. Synth. Process.*, 2000, **8**(3–4), 181–188.
29 L. Takacs, Gradual and self-sustaining processes in the Sn-Zn-Se system, *Acta Phys. Pol., A*, 2014, **126**(4), 1032–1039.
30 L. Takacs and M. A. Susol, Gradual and combustive mechanochemical reactions in the Sn-Zn-S system, *J. Solid State Chem.*, 1996, **121**(2), 394–399.
31 F. Torre, M. Carta, P. Barra, A. Cincotti, A. Porcheddu and F. Delogu, Mechanochemical Ignition of Self-propagating

Reactions in Zn-S Powder Mixtures, *Metall. Mater. Trans. B*, 2021, **52**(2), 830–839.
32 M. A. Aviles, J. M. Cordoba, M. J. Sayagues and F. J. Gotor, Tailoring the Band Gap in the ZnS/ZnSe System: Solid Solutions by a Mechanically Induced Self-Sustaining Reaction, *Inorg. Chem.*, 2019, **58**(4), 2565–2575.
33 M. A. Aviles and F. J. Gotor, Tuning the excitation wavelength of luminescent Mn2+-doped ZnSxSe1-x obtained by mechanically induced self-sustaining reaction, *Opt. Mater.*, 2021, **117**, 111121.
34 L. Takacs, Self-sustaining reactions as a tool to study mechanochemical activation, *Faraday Discuss.*, 2014, **170**, 251–265.
35 T. Ohtani, Y. Kusano, K. Ishimaru, T. Morimoto, A. Togano and T. Yoshioka, Pre-milling effects on self-propagating reactions in mechanochemical synthesis of CdSe and ZnSe, *Chem. Lett.*, 2015, **44**(9), 1234–1236.
36 M. Baláž, A. Zorkovská, F. Urakaev, P. Baláž, J. Briančin, Z. Bujňáková, M. Achimovičová and E. Gock, Ultrafast mechanochemical synthesis of copper sulfides, *RSC Adv.*, 2016, **6**(91), 87836–87842.
37 L. Takacs, Ball milling-induced combustion in powder mixtures containing titanium, zirconium, or hafnium, *J. Solid State Chem.*, 1996, **125**(1), 75–84.
38 D. Tetzlaff, K. Pellumbi, D. M. Baier, L. Hoof, H. S. Barkur, M. Smialkowski, H. M. Amin, S. Grätz, D. Siegmund and L. Borchardt, Sustainable and rapid preparation of nanosized Fe/Ni-pentlandite particles by mechanochemistry, *Chem. Sci.*, 2020, **11**(47), 12835–12842.
39 S. Wu, Y. Xue and Z. Zhang, Microanalysis on CuInSe2 compound synthesized by mechanochemical processing, *J. Alloys Compd.*, 2010, **491**(1–2), 456–459.
40 S. M. Wu, Y. Z. Xue, L. M. Zhou, X. Liu and D. Y. Xu, Structure and morphology evolution in mechanochemical processed $CuInS_2$ powder, *J. Alloys Compd.*, 2014, **600**, 96–100.
41 S. Wu, Y. Liang, L. Zhou, X. Liu, C. Mao and Y. Teng, Influence of S content on the structure and ignition time of CuIn(S,Se)2 powders prepared by mechanochemical process, *J. Alloys Compd.*, 2018, **731**, 318–322.
42 L. Caggiu, S. Enzo, L. Stievano, R. Berthelot, C. Gerbaldi, M. Falco, S. Garroni and G. Mulas, Solvent-Free Mechanochemical Approach towards Thiospinel MgCr2S4 as a Potential Electrode for Post-Lithium Ion Batteries, *Batteries*, 2020, **6**(3), 43.
43 P. Baláž, M. Baláž, M. J. Sayagués, A. Eliyas, N. G. Kostova, M. Kaňuchová, E. Dutková and A. Zorkovská, Chalcogenide quaternary Cu_2FeSnS_4 nanocrystals for solar cells: Explosive character of mechanochemical synthesis and environmental challenge, *Crystals*, 2017, **7**(12), 367.
44 F. J. Gotor, M. Achimovičová, C. Real and P. Baláž, Influence of the milling parameters on the mechanical work intensity in planetary mills, *Powder Technol.*, 2013, **233**, 1–7.
45 F. K. Urakaev, Experimental study of mechanically induced self-propagating reactions in metal-sulfur mixtures, *Combust. Sci. Technol.*, 2013, **185**(3), 473–483.
46 L. Takacs, Self-Sustaining Reactions Induced by Ball Milling: An Overview, *Int. J. Self-Propag. High-Temp. Synth.*, 2009, **18**(4), 276–282.
47 R. Ebrahimi-Kahrizsangi, M. Abdellahi and M. Bahmanpour, Self-ignited synthesis of nanocomposite powders induced by Spex mills; modeling and optimizing, *Ceram. Int.*, 2015, **41**(2), 3137–3151.
48 R. Ebrahimi-Kahrizsangi, M. Abdellahi and M. Bahmanpour, Mechanically Induced Self-Sustaining Reactions, *Int. J. Self-Propag. High-Temp. Synth.*, 2016, **25**(1), 5–13.
49 L. Takacs and M. A. Susol, Combustive mechanochemical reactions in off-stoichiometric powder mixtures, *Mater. Sci. Forum*, 1996, **225–227**, 559–562.
50 Y. F. Yang, H. Y. Wang, R. Y. Zhao, Y. H. Liang, L. Zhan and Q. C. Jiang, Effects of C particle size on the ignition and combustion characteristics of the SHS reaction in the 20 wt.% Ni-Ti-C system, *J. Alloys Compd.*, 2008, **460**(1–2), 276–282.
51 O. Coban, M. Bugdayci, S. Baslayici and M. E. Acma, Combustion Synthesis of B4C-TiB Nanocomposite Powder: Effect of Mg Particle Size on SHS and Optimization of Acid Leaching Process, *J. Superhard Mater.*, 2023, **45**(1), 20–30.
52 G. V. Samsonov, *Handbook of the Physicochemical Properties of the Elements*, Springer, New York, 1968, p. 942.
53 M. K. Karapet'yans and M. L. Karapet'yans, *Thermodynamic Constants of Inorganic and Organic Compounds*, Humphrey Science Publishers, Ann Arbor, 1970, p. 461.
54 V. P. Skripov, V. P. Koverda and V. N. Skokov, Size Effect on Melting of Small Particles, *Phys. Status Solidi A*, 1981, **66**(1), 109–118.
55 M. A. Ansari, Modelling of size-dependent thermodynamic properties of metallic nanocrystals based on modified Gibbs-Thomson equation, *Appl. Phys. A*, 2021, **127**(5), 385.
56 D. R. Lide, *CRC Handbook of Chemistry and Physics*; CRC Press, Boca Raton, 85th edn, 2004-2005.
57 D. J. Vaughan and J. R. Craig, *Mineral Chemistry of Metal Sulfides*, Cambridge University Press, Cambridge, 1978, p. 493.
58 O. Zobac, K. Buchlovska, J. Pavlu and A. Kroupa, Thermodynamic Description of Binary System Nickel-Selenium, *J. Phase Equilib. Diffus.*, 2021, **42**(4), 468–478.
59 S. Deore, F. Xu and A. Navrotsky, Oxide-melt solution calorimetry of selenides: Enthalpy of formation of zinc, cadmium, and lead selenide, *Am. Mineral.*, 2008, **93**(5–6), 779–783.
60 I. Barin, *Thermochemical Data of Pure Substances*, VCH, Weinheim, 1981, p. 1829.
61 A. M. James and M. P. Lord, *Macmillan's Chemical and Physical Data*, Macmillan, London, UK, 1992.
62 G. W. C. Kaye and T. H. Laby, *Tables of Physical and Chemical Constants*, Longman, London, UK, 15th edn, 1993, p. 477.
63 E. G. Avvakumov and N. V. Kosova, Fast Propagating Solid-State Mechanochemical Reactions, *Sib. Khim. Zh.*, 1991, **5**, 62–66.
64 Z. A. Munir and U. Anselmi-Tamburini, Self-propagating exothermic reactions: The synthesis of high-temperature materials by combustion, *Mater. Sci. Rep.*, 1989, **3**(7–8), 277–365.

65 L. Takacs, Combustion phenomena induced by ball milling, *Mater. Sci. Forum*, 1998, **269–2**, 513–522.
66 A. A. L. Michalchuk, The Thermodynamics and Kinetics of Mechanochemical Reactions, in *Mechanochemistry and Emerging Technologies for Sustainable Chemical Manufacturing*, ed. Colacino, E. and Garcia, F., CRC Press, Boca Raton, 2023, p. 34.
67 P. A. Thiessen, G. Heinicke and E. Schober, To the tribochemical reaction of gold and CO_2 with the aid of radioactive labeling (in German), *Z. Anorg. Allg. Chem.*, 1970, **377**, 20–28.
68 A. A. Coelho, TOPAS and TOPAS-Academic: an optimization program integrating computer algebra and crystallographic objects written in C plus, *J. Appl. Crystallogr.*, 2018, **51**, 210–218.
69 J. S. O. Evans, Advanced Input Files & Parametric Quantitative Analysis Using Topas, *Mater. Sci. Forum*, 2010, **651**, 1–9.